Partial-wave analysis of $\tau^{\mp} \to \pi^{\mp}\pi^{\mp}\pi^{\pm}\nu_{\tau}$

BELLE collaboration

Andrei Rabusov, Daniel Greenwald, and Stephan Paul

Technical University of Munich

HADRON 2023

June 8th Genova

$\tau^- \to \pi^-\pi^-\pi^+\nu_\tau$: Motivation

* Phys.Rev. Lett. 115, 082001

Searches for new particles and interactions not part of the Standard Model: need to know various hadron form-factors

Disagreement in measurements of $\mathrm{a}_1(1260)$ parameters

- COMPASS observed* narrow peak $\mathrm{a}_1(1420)$
  - Isospin partner of $\mathrm{f}_1(1420)$?
  - $\mathrm{K}^*\mathrm{K}$ rescattering?
- $\tau \to 3\pi\nu$ provides X-check for COMPASS 3π partial wave analysis (PWA) in different experimental conditions

Improve current model in event generators

$\mathrm{a}_1(1420)$ observation at COMPASS

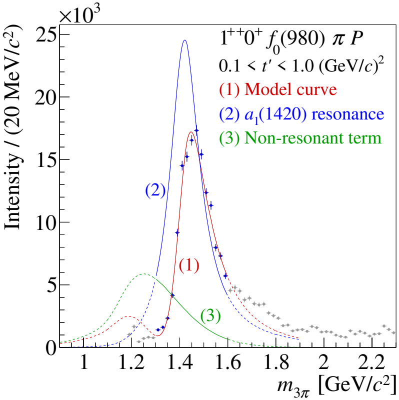

$\tau^- \to \pi^-\pi^-\pi^+\nu_\tau$: Motivation

Searches for new particles and interactions not part of the Standard Model: need to know various hadron form-factors

Disagreement in measurements of $\mathrm{a}_1(1260)$ parameters

- COMPASS observed* narrow peak $\mathrm{a}_1(1420)$
  - Isospin partner of $\mathrm{f}_1(1420)$?
  - $\mathrm{K}^*\mathrm{K}$ rescattering?
- $\tau \to 3\pi\nu$ provides X-check for COMPASS 3π partial wave analysis (PWA) in different experimental conditions

Improve current model in event generators

$\mathrm{a}_1(1420)$ observation at COMPASS

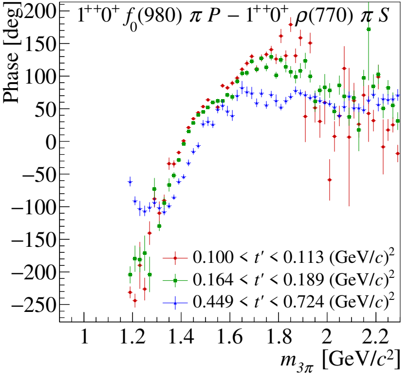

BELLE@KEKB

KEKB is asymmetric e^+e^- collider

$E_{e^+} = 3.5$ GeV, $E_{e^-} = 8$ GeV

Total luminosity: 988 fb^{-1}

- $\Upsilon(4S)$: 711 fb^{-1}
- 0.9×10^9 tauon pairs produced

Tauon:

- $m = 1.777$ MeV
- $c\tau = 86$ µm
- $\mathcal{B}(\tau^\mp\pi^\mp\pi^\mp\pi^\pm\nu_\tau) = 9\%$

Integrated luminosity of Belle

Event-selection criteria

Event-class selection

- Standard Belle selection for tauon pairs
- Topology: 3–1
- Boosted Decision Tree

Signal hemisphere

- Tracks identification:
  - Veto signal-side particles being electrons or muons
  - Veto the like-sign signal-side particles being kaons
- Veto pions coming from K$_0$: $\left|m_{2\pi} - m_{\mathrm{K_S}}\right| < 12$ MeV
- Veto π^0s in signal hemisphere: $\sum E_\gamma < 480$ MeV

Event-selection criteria

Selection criteria summary:

	Previous*	Current
Efficiency	22 %	32 %
Purity	89 %	82 %
# of events	9×10^6	55×10^6

Major background components:

$\tau \to 3\pi^{\mp}\pi^0\nu_\tau$	12 %
$e^+e^- \to q\bar{q}$	4 %
$\tau \to K^{\mp}2\pi^{\mp}\nu_\tau$	1 %
$\tau \to 3\pi^{\mp}N\pi^0\nu_\tau, N \geq 2$	0.8 %

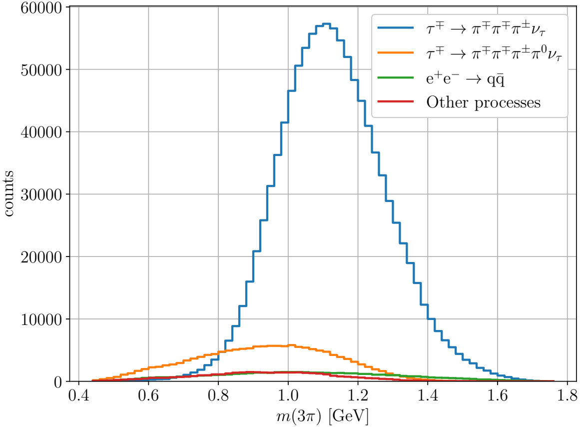

Simulated $m_{3\pi}$ spectrum

Phase space

Assume $\pi_3 = \pi^+$, π_1 and π_2 denote π^-s.

Four-body decay: 7 free parameters

- $q^2 = m_{3\pi}^2$
- $s_1 = m_{23}^2$, $s_2 = m_{13}^2$
- θ: angle between hadron system and $-\hat{n}_{\text{CMS}}$ in tau frame — helicity angle
- α, β, and γ: Euler angles of basis transformation in hadron frame from “lepton“ basis to “hadron“ basis

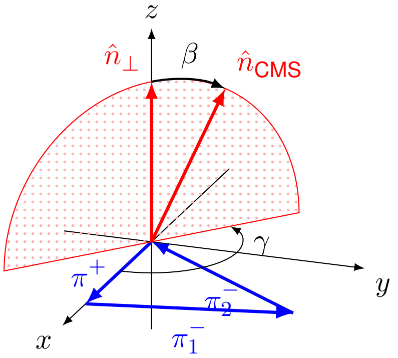

Euler angles in hadron rest frame

Matrix element

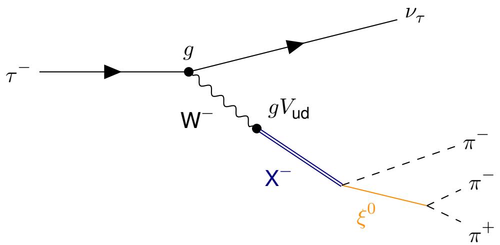

Matrix element

* Eur.Phys.J.C 81 (2021) 12, 1073

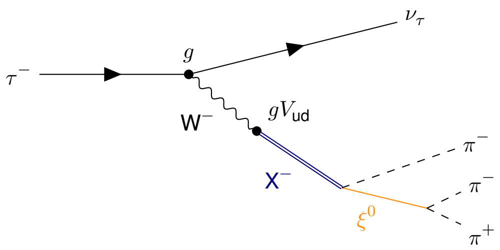

Average intensity over α because tauon direction can't be measured

Matrix element

* Eur.Phys.J.C 81 (2021) 12, 1073

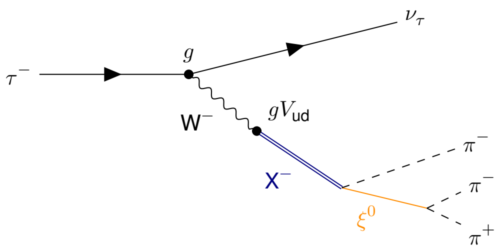

Average intensity over α because tauon direction can't be measured

Decompose hadron current* J^μ_{had} into partial waves

Matrix element

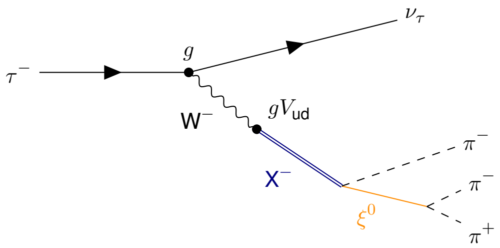

Average intensity over α because tauon direction can't be measured

Decompose hadron current* J^μ_{had} into partial waves

$$J^\mu_{\mathrm{had}} = \sum_w \mathcal{C}_w j^\mu_w$$

Matrix element

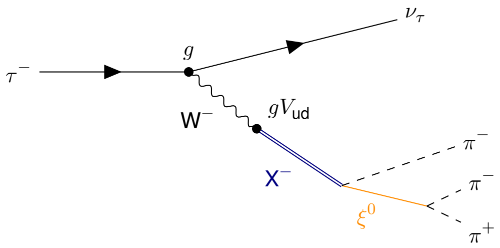

Average intensity over α because tauon direction can't be measured

Decompose hadron current* J^μ_{had} into partial waves

$$J^P[\xi^0\pi]_L$$

Partial waves

* 2305.11711 [hep-ph]

Partial wave	$m(\xi)$ [GeV]	$\Gamma(\xi)$ [GeV]	Threshold [GeV]
$1^+[\sigma\pi]_\mathrm{P}$	Broad $[\pi\pi]_\mathrm{S}$-wave component*		
$1^+[\mathrm{f}_0(980)\pi]_\mathrm{P}$	0.990	0.07	1.14
$1^+[\mathrm{f}_0(1500)\pi]_\mathrm{P}$	1.504	0.109	1.24
$1^+[\rho(770)\pi]_\mathrm{S}$	0.769	0.1509	—
$1^+[\rho(770)\pi]_\mathrm{D}$			—
$1^+[\rho(1450)\pi]_\mathrm{S}$	1.465	0.40	1.18
$1^+[\rho(1450)\pi]_\mathrm{D}$			1.0
$1^+[\mathrm{f}_2(1270)\pi]_\mathrm{P}$	1.2755	0.1867	1.1
$1^+[\mathrm{f}_2(1270)\pi]_\mathrm{F}$			1.06
$0^-[\sigma\pi]_\mathrm{S}$			—
$0^-[\mathrm{f}_0(980)\pi]_\mathrm{S}$			1.14
$0^-[\rho(770)\pi]_\mathrm{P}$			—
$0^-[\mathrm{f}_2(1270)\pi]_\mathrm{D}$			1.0

Partial wave	Threshold [GeV]
$1^-[\rho(770)\pi]_\mathrm{P}$	—
$1^-[\mathrm{f}_2(1270)\pi]_\mathrm{D}$	—
$1^+[\omega(782)\pi]_\mathrm{S}$	1.0

Spin-exotic or “obscure” partial waves

Fitting strategies

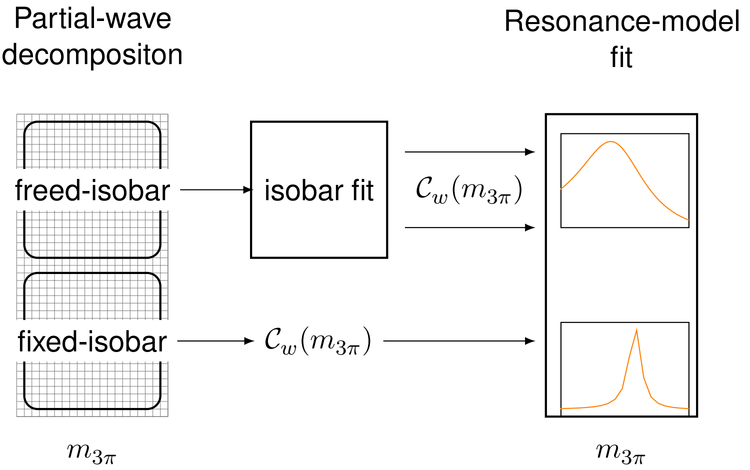

Fitting strategies

Conventional PWA:

- Isobars shape is fixed
- Fit in bins of $m_{3\pi}$ (no a$_1$ shape assumptions)
- $2 \times N_{\text{PW}} - 1$ free parameters: partial-waves complex coefficients $\mathcal{C}_w$ (one phase is fixed)

Intensity:

$$\mathcal{I} = \sum_{w,v} \mathcal{C}_w \mathcal{C}_v^* \mathcal{I}_{w\,v}$$

$$\mathcal{I}_{w\,v} = \overline{\mathcal{L}_{\mu\nu}} j_w^{\mu} \left(j_v^{\nu}\right)^*$$

Extended log likelihood function:

$$\ln \mathcal{L} = \sum_{\text{Data}} \ln \sum_{w,v} \mathcal{C}_w \mathcal{C}_v^* \mathcal{I}_{w\,v} - \sum_{w,v} \mathcal{C}_w \mathcal{C}_v^* \mathcal{N}_{w\,v}$$

Integral matrix:

$$\mathcal{N}_{wv} = \frac{\sum\limits_{\text{Acc MC}} \mathcal{I}_{wv} / \left|\mathcal{M}_{\text{MC Generator}}\right|^2}{\sum\limits_{\text{Acc MC}} 1 / \left|\mathcal{M}_{\text{MC Generator}}\right|^2}$$

$\left|\mathcal{M}_{\text{MC Generator}}\right|^2$ `TAUOLA` intensity (CLEO current for $\tau \to 3\pi\nu_\tau$)

Comparison of simulation with data

Slice of $m_{3\pi} \in [1.50, 1.52]$ GeV

Fit to $20\% L_{\text{int}}$ data and simulate $\tau^{\mp} \to \pi^{\mp}\pi^{\mp}\pi^{\pm}\nu_{\tau}$

Plot legend:

- Black dots: data
- Blue hist: Fit prediction with `TAUOLA-m`
- Orange hist: background

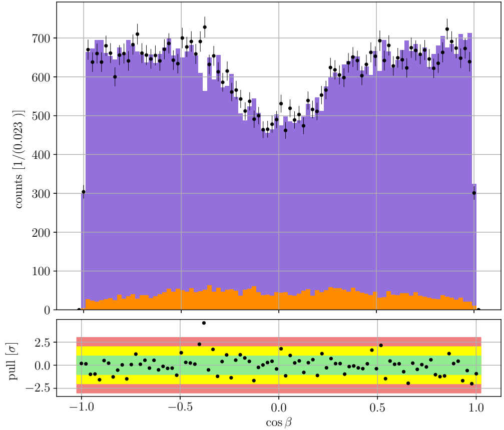

$\cos\beta$

Comparison of simulation with data

Slice of $m_{3\pi} \in [1.50, 1.52]$ GeV

Fit to $20\% L_{\text{int}}$ data and simulate $\tau^{\mp} \to \pi^{\mp}\pi^{\mp}\pi^{\pm}\nu_{\tau}$

Plot legend:

- Black dots: data
- Blue hist: Fit prediction with `TAUOLA-m`
- Orange hist: background

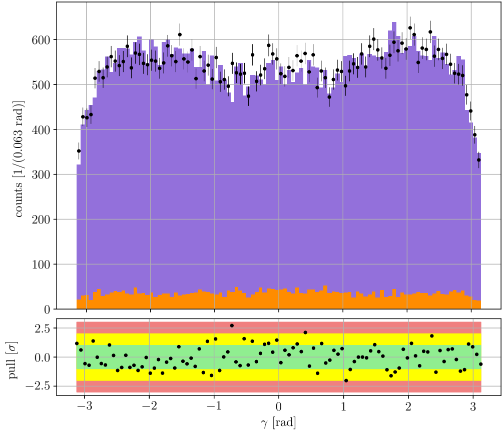

γ

Comparison of simulation with data

Slice of $m_{3\pi} \in [1.50, 1.52]$ GeV

Fit to $20\% L_{\text{int}}$ data and simulate $\tau^{\mp} \to \pi^{\mp}\pi^{\mp}\pi^{\pm}\nu_{\tau}$

Plot legend:

- Black dots: data
- Blue hist: Fit prediction with `TAUOLA-m`
- Orange hist: background

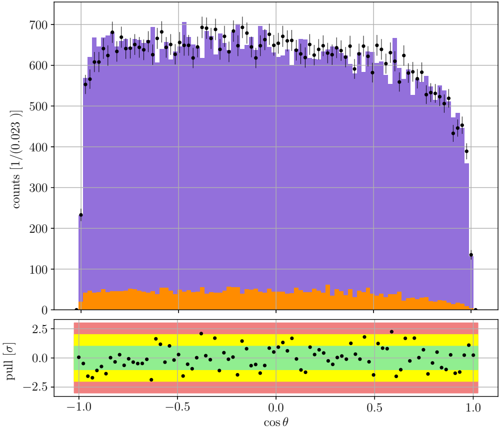

$\cos\theta$

Comparison of simulation with data

Slice of $m_{3\pi} \in [1.50, 1.52]$ GeV

Fit to $20\% L_{\text{int}}$ data and simulate $\tau^{\mp} \to \pi^{\mp}\pi^{\mp}\pi^{\pm}\nu_{\tau}$

Plot legend:

- Black dots: data
- Blue hist: Fit prediction with `TAUOLA-m`
- Orange hist: background

Data overshoots simulation at the $\rho(770)$ peak position

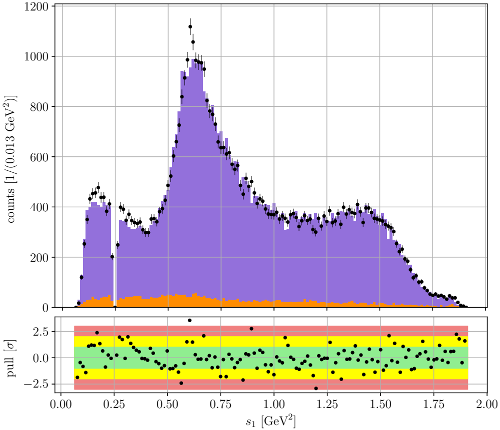

s_1 [GeV^2]

Comparison of simulation with data

Slice of $m_{3\pi} \in [1.50, 1.52]$ GeV

Fit to $20\% L_{\text{int}}$ data and simulate $\tau^{\mp} \to \pi^{\mp}\pi^{\mp}\pi^{\pm}\nu_{\tau}$

Plot legend:

- Black dots: data
- Blue hist: Fit prediction with `TAUOLA-m`
- Orange hist: background

Data overshoots simulation at the $\rho(770)$ peak position

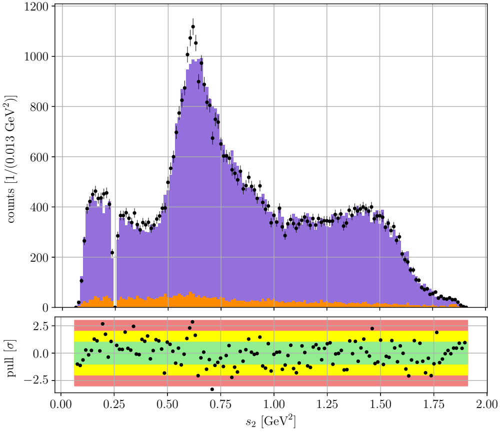

s_2 [GeV^2]

Significance of $\mathrm{a}_1(1420)$

Resonance-model fit, $\chi^2/\mathrm{ndf} = 60.48/24$ for the $1^+[\mathrm{f}_0(980)\pi]_\mathrm{P}$ intensity.

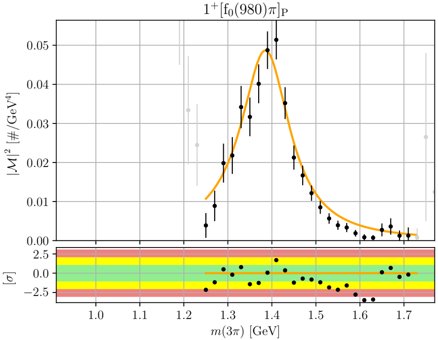

$1^+[\mathrm{f}_0(980)\pi]_\mathrm{P}$ intensity. Orange curve shows the resonance-model fit projection

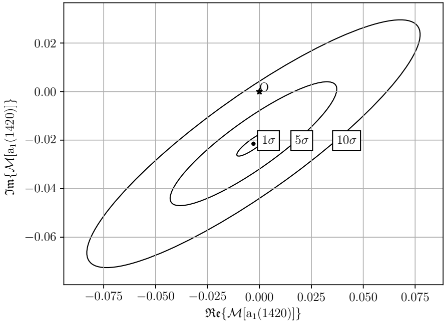

Complex magnitude of $\mathrm{a}_1(1420)$ decaying to $1^+[\mathrm{f}_0(980)\pi]_\mathrm{P}$, ellipses show confidence intervals

Systematic effects: overview

Four major sources:

- Model:
  - Isobar parametrization
  - Model selection
- Background
  - Model in simulations
  - Neural network parametrization
- Acceptance
  - Stat. uncertainty of $\mathcal{N}_{wv}$
  - Momentum correction
- Detector resolution

Background

Neural network* trained on simulated data

Neural network shape fixed in PWA

Test background leakage on simulated data

Background still leaks to signal

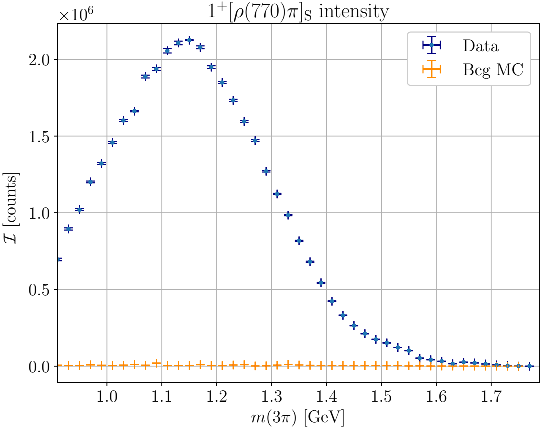

Background

* JINST 16 (2021) 06, P06016

- Neural network* trained on simulated data
- Neural network shape fixed in PWA
- Test background leakage on simulated data
- Background still leaks to signal

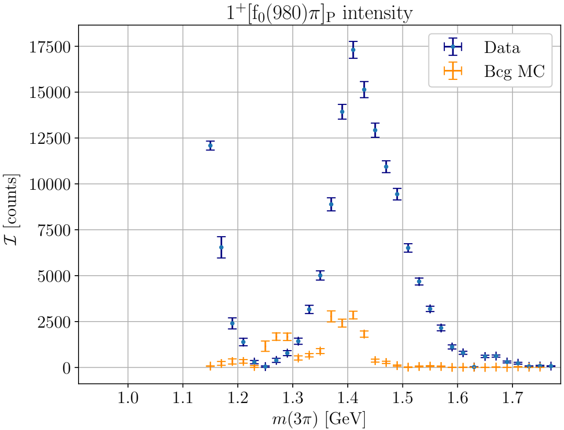

Neural network uncertainty:

Plots' legend:

- Stat. uncertainty
- Syst. uncertainty

Propagate uncertainties by varying neural network parameters before PWA

25–120 networks/bin

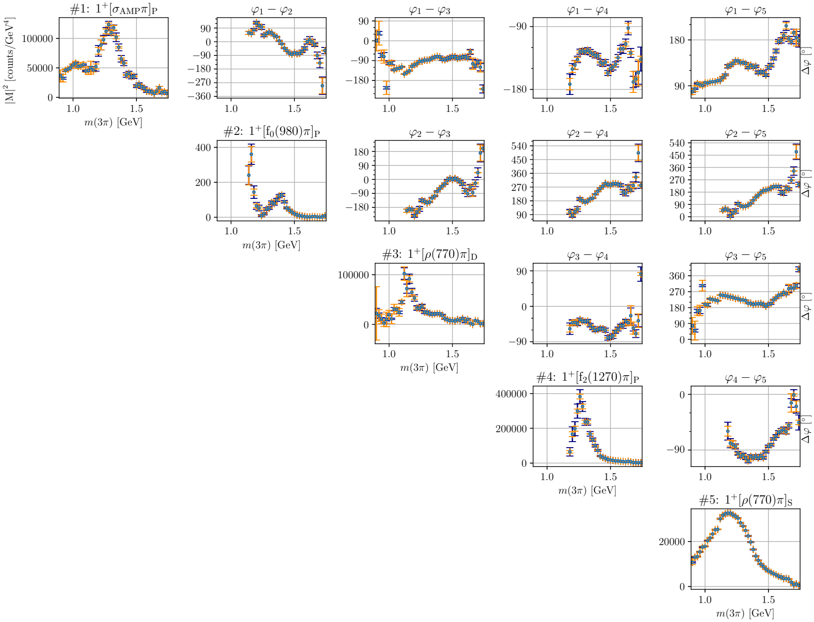

Integrals uncertainty:

Plots' legend:

- Stat. uncertainty
- Syst. uncertainty

Propagate statistical uncertainties of integrals by varying integrals within their statistical uncertainties before PWA

Correlations not taken into account

$100\ \mathcal{N}_{wv}$/bin

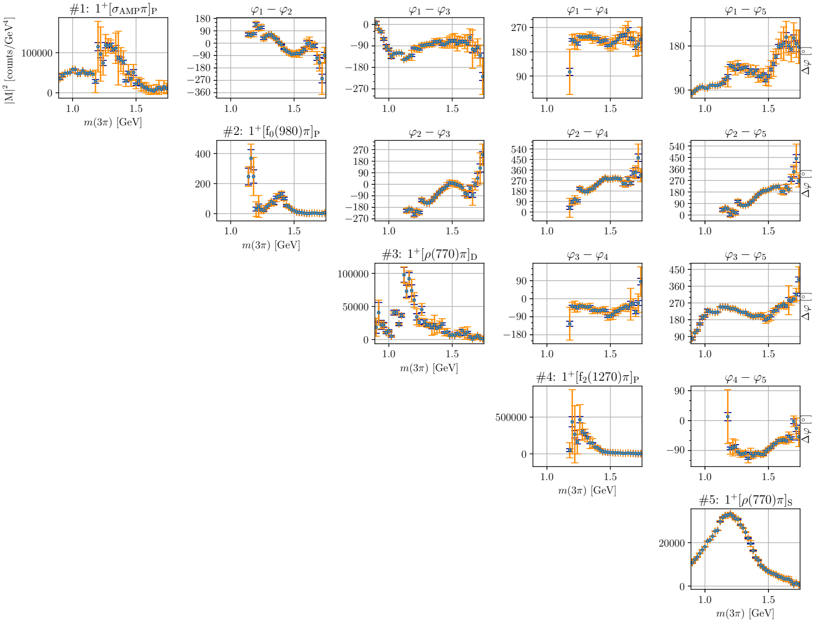

Summary and plans

Current status:

- Selection criteria
- Background description with neural network
- Partial-wave decomposition
  - Fixed-isobar
  - Freed-isobar
- Resonance-model and isobar fits
- Systematic uncertainties:
  - Model
  - Background
  - Acceptance
  - Resolution

Preliminary results:

- $\mathrm{a}_1(1420)$ is discovered in tau decays

Remaining systematic studies:

- Background model
- Trigger
- PID

Plans:

- Extract $\mathrm{a}_1(1260)$ pole parameters
- Test for exotic mesons
- Publish this year

Thank you for your attention!

Backup

List of selections

Good tracks selection:

- $|\Delta r| < 0.5$ cm
- $|\Delta z| < 2.5$ cm
- $p_\perp > 0.1$ GeV

Good photons selection:

- $E_\gamma > 0.04$ GeV
- $w > 0.5$ cm
- $N_{\text{hits}} > 2$
- $E_{\text{seed}}/E_{\text{cluster}} < 0.95$

Preselection: four good tracks with sum charge zero

Skimming:

- `tau_skimB` or `HadronBJ`
- BDT response $b_{\tau\tau} > 0$

Topology: $3 + 1$

Loose π^0-veto in signal hemisphere: $\sum E_\gamma < 0.48$ GeV

Signal tracks PID:

- three tracks: e-veto, μ-veto
- two tracks same charge: K-veto

$\mathrm{K_S}$-veto in signal hemisphere: $\left|m_{2\pi} - m_{\mathrm{K_S}}\right| < 0.012$ GeV

Event display

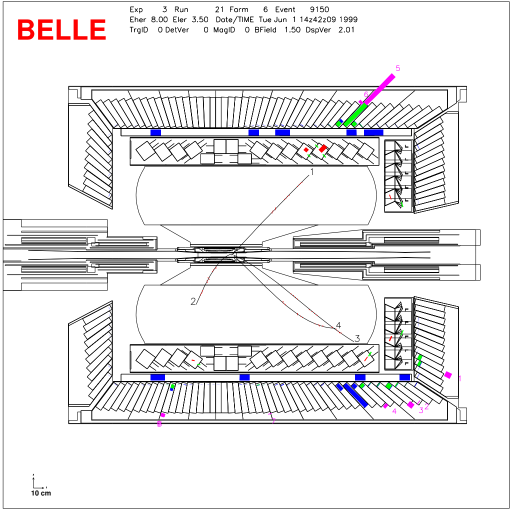

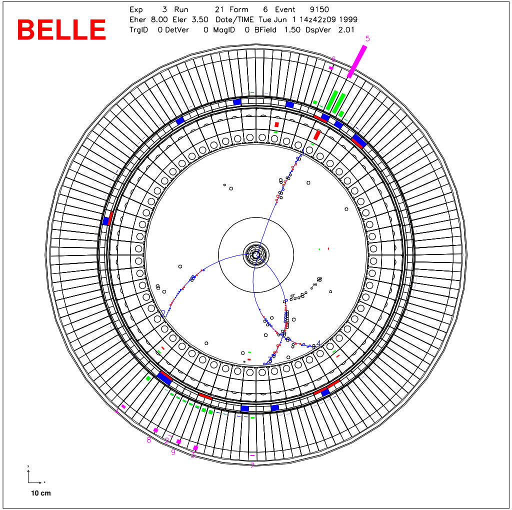

Efficiency and purity

Sequential efficiencies and purities:

Criterion	purity [%]	efficiency [%]
baseline	22.1	44.4
trig	23.1	43.8
skim	24.5	43.1
BDT	50.6	39.9
LID	54.0	37.8
HID	57.4	36.7
PHS	57.7	36.7
ISR	58.2	35.9
KS_veto	60.7	34.3
pi0_veto	81.6	32.3

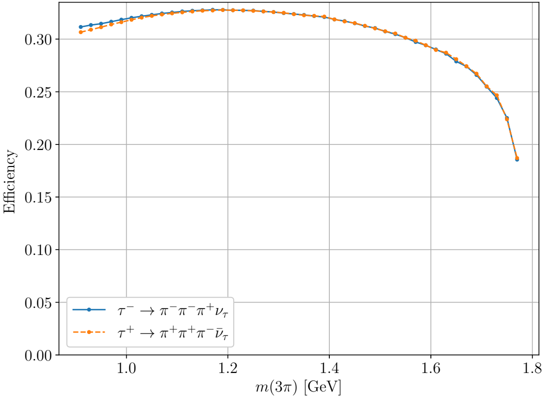

$m(3\pi)$ efficiency

Efficiency and purity

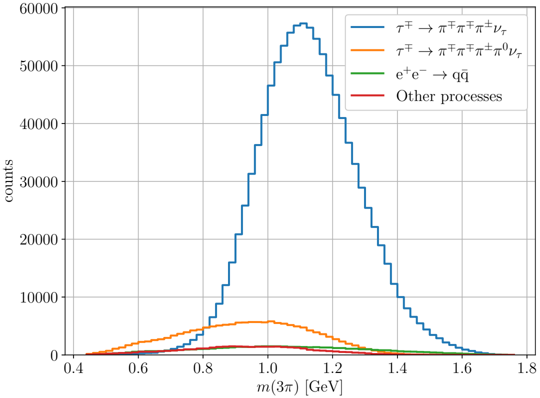

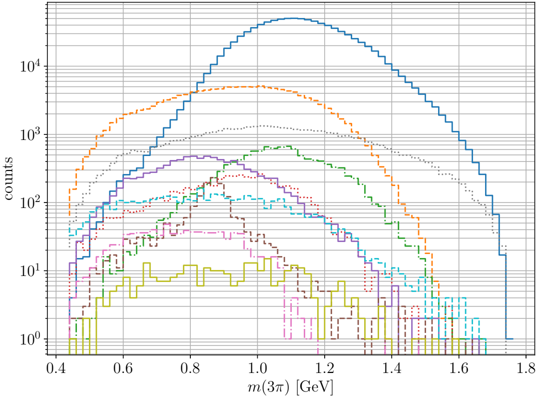

$m(3\pi)$ spectrum in MC

$m(3\pi)$ spectrum in MC, $\log\mathrm{OY}$

Freed isobar PWA

Conventional PWA:

- Isobar's shape $\Delta(s)$ is fixed
- One complex coefficient $\mathcal{C}_w$ per wave

Breit-Wigner (BW) parametrization:

$$\Delta_\xi(s) = \mathrm{BW}_\xi(s) = \frac{m_\xi^2}{m_\xi^2 - s - i\sqrt{s}\Gamma(s)}$$

$$\Gamma_\xi(s) = \Gamma_\xi \left(\frac{q_s}{q_m}\right)^{2L_\xi+1} \frac{m_\xi}{\sqrt{s}}$$

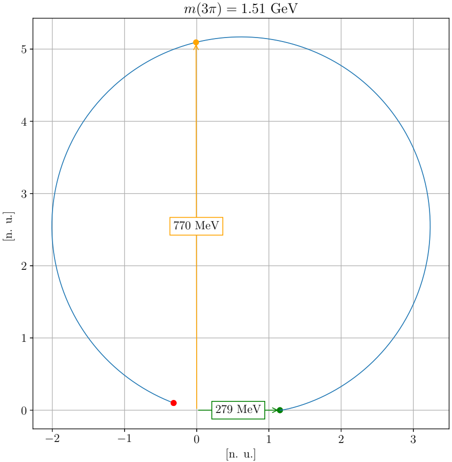

Argand plot: $\rho(770)$ BW

Freed isobar PWA

Freed isobar PWA:

$$\Delta(s) = \sum_{w\,\text{freed}} \mathcal{C}_{w\,\text{freed}} \Theta_w(s)$$

$$\Theta_w(s) = \begin{cases} 1 & \text{if } s \text{ in the } m_{2\pi} \text{ bin } w \\ 0 & \text{otherwise} \end{cases}$$

1^{--} $m(2\pi)$ binning:

$$\begin{cases} 20\ \text{MeV} & [640, 920]\ \text{MeV} \\ 40\ \text{MeV} & \text{otherwise} \end{cases}$$

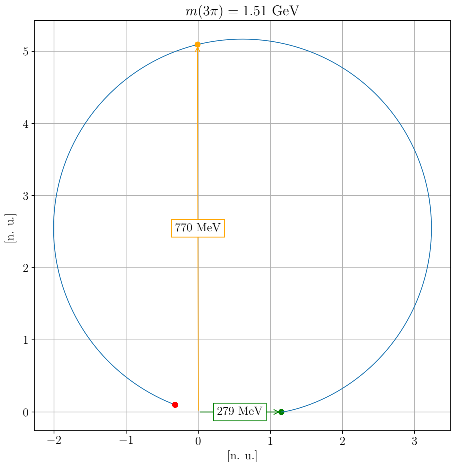

Argand plot: $\rho(770)$ BW

Freed isobar PWA

Freed isobar PWA:

$$\Delta(s) = \sum_{w\,\text{freed}} \mathcal{C}_{w\,\text{freed}} \Theta_w(s)$$

$$\Theta_w(s) = \begin{cases} 1 & \text{if } s \text{ in the } m_{2\pi} \text{ bin } w \\ 0 & \text{otherwise} \end{cases}$$

0^{++} $m(2\pi)$ binning:

$$\begin{cases} 10\text{ MeV} & [920, 1080]\text{ MeV} \\ 40\text{ MeV} & \text{otherwise} \end{cases}$$

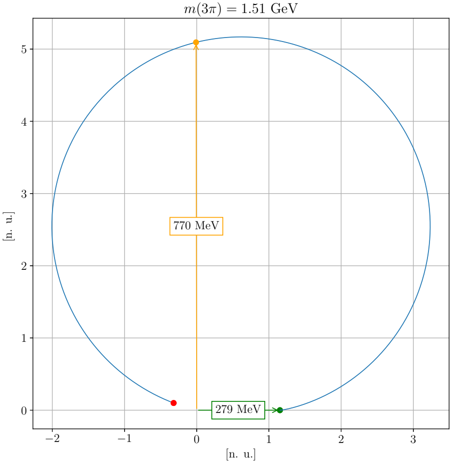

Argand plot: $\rho(770)$ BW

Freed isobar PWA

Freed isobar PWA:

$$\Delta(s) = \sum_{w \text{ freed}} \mathcal{C}_{w \text{ freed}} \Theta_w(s)$$

$$\Theta_w(s) = \begin{cases} 1 & \text{if } s \text{ in the } m_{2\pi} \text{ bin } w \\ 0 & \text{otherwise} \end{cases}$$

Mathematical ambiguities (zero modes)

`10.1103/PhysRevD.97.114008`

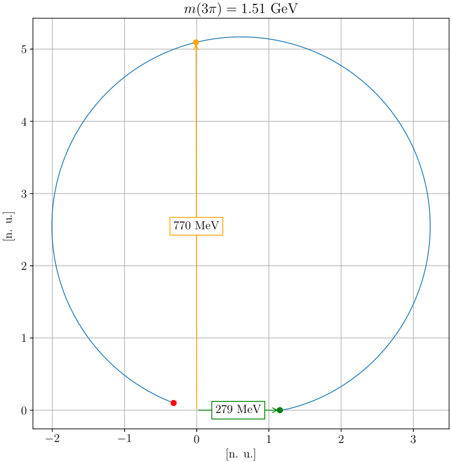

Argand plot: $\rho(770)$ BW

Isobar fit

$1^+[0^{++}\pi]_\mathrm{P}$ wave

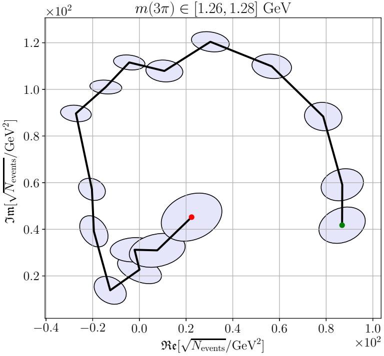

$1^+[1^{--}\pi]_\mathrm{S}$ wave

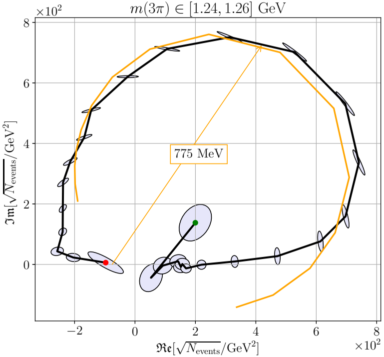

$m_{3\pi} \in [1.24, 1.26]$ GeV

Isobar fit

$1^+[0^{++}\pi]_P$ wave

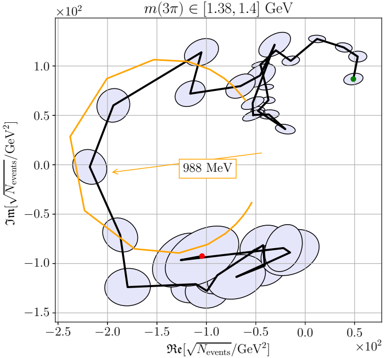

$1^+[1^{--}\pi]_S$ wave

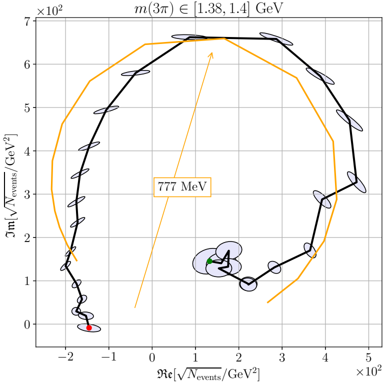

$m_{3\pi} \in [1.38, 1.40]$ GeV

Isobar fit

$1^{+}[0^{++}\pi]_{\mathrm{P}}$ wave

Extracted $1^{+}[\mathrm{f}_0(980)\pi]_{\mathrm{P}}$ wave parameters:

m	988.0 ± 2.5 [MeV]
m PDG 2022	980 ± 20 [MeV]
Γ	49.5 ± 5.2 [MeV]
Γ PDG 2022	50–100 [MeV]
$\mathfrak{Re}$	-0.4 ± 1.3 [$\sqrt{N}$/GeV^2]
$\mathfrak{Im}$	9.8 ± 1.1 [$\sqrt{N}$/GeV^2]

$1^{+}[1^{--}\pi]_{\mathrm{S}}$ wave

Extracted $1^{+}[\rho(770)\pi]_{\mathrm{S}}$ wave parameters:

m	777.0 ± 1.0 [MeV]
m PDG 2022	775.26 ± 0.25 [MeV]
Γ	139.6 ± 2.3 [MeV]
Γ PDG 2022	149.1 ± 0.8 [MeV]
$\mathfrak{Re}$	113.6 ± 2.6 [$\sqrt{N}$/GeV^2]
$\mathfrak{Im}$	25.1 ± 5.2 [$\sqrt{N}$/GeV^2]

$m_{3\pi} \in [1.38, 1.40]$ GeV

Freed result in $m_{3\pi}$

Clear peak at 1.4 GeV in $1^{+}[\mathrm{f}_0(980)\pi]_{\mathrm{P}}$-wave

Clear phase motion at 1.4 GeV in $1^{+}[\mathrm{f}_0(980)\pi]_{\mathrm{P}}$-wave

$\mathrm{a}_1(1260)$ is dominant in the $1^{+}[\rho(770)\pi]_{\mathrm{S}}$-wave

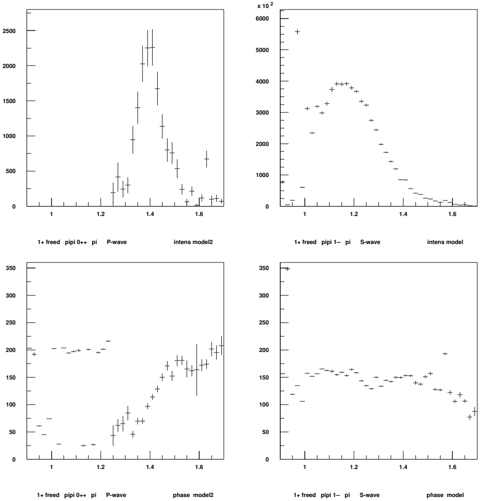

Blatt-Weisskopf centrifugal-barrier factor F

F takes into the finite size of a meson

Each partial wave is multiplied by two Fs corresponding to either X^- or ξ^0

F_S for ξ^0 depends on the break-up momentum in the rest frame of ξ^0

F_L for X^- depends on the break-up momentum in the rest frame of X^-

There are two alternative parametrizations for F, I use the relativistic one, for example for a P wave

$$F_P(x) = \sqrt{\frac{1 - x_0}{1 - x}}, \; x = (pd)^2$$

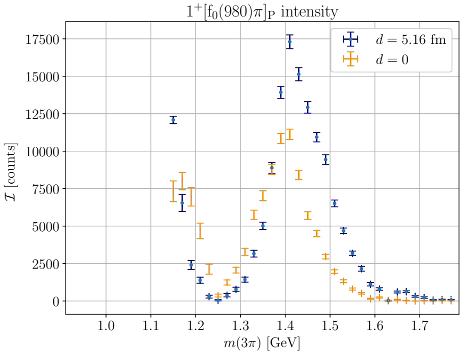

Blatt-Weisskopf centrifugal-barrier factor F

- F takes into the finite size of a meson
- Each partial wave is multiplied by two Fs corresponding to either X^- or ξ^0
- F_S for ξ^0 depends on the break-up momentum in the rest frame of ξ^0
- F_L for X^- depends on the break-up momentum in the rest frame of X^-
- There are two alternative parametrizations for F, I use the relativistic one, for example for a P wave

$$F_P(x) = \sqrt{\frac{1 - x_0}{1 - x}}, \; x = (pd)^2$$

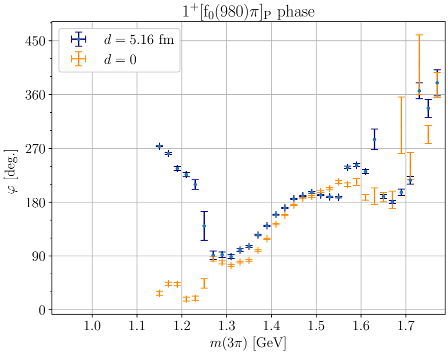

Blatt-Weisskopf centrifugal-barrier factor F

F takes into the finite size of a meson

Each partial wave is multiplied by two Fs corresponding to either X$^-$ or ξ^0

F_S for ξ^0 depends on the break-up momentum in the rest frame of ξ^0

F_L for X$^-$ depends on the break-up momentum in the rest frame of X$^-$

There are two alternative parametrizations for F, I use the relativistic one, for example for a P wave

$$F_P(x) = \sqrt{\frac{1 - x_0}{1 - x}}, \; x = (pd)^2$$

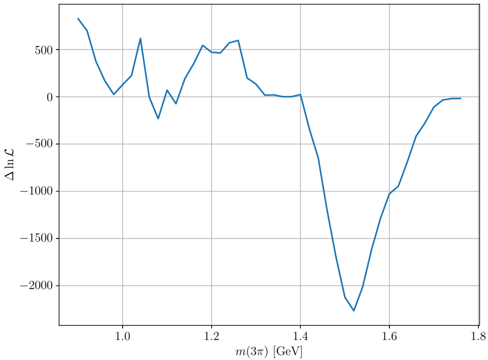

Difference between $\ln \mathcal{L}$ of the fit.

1D projections

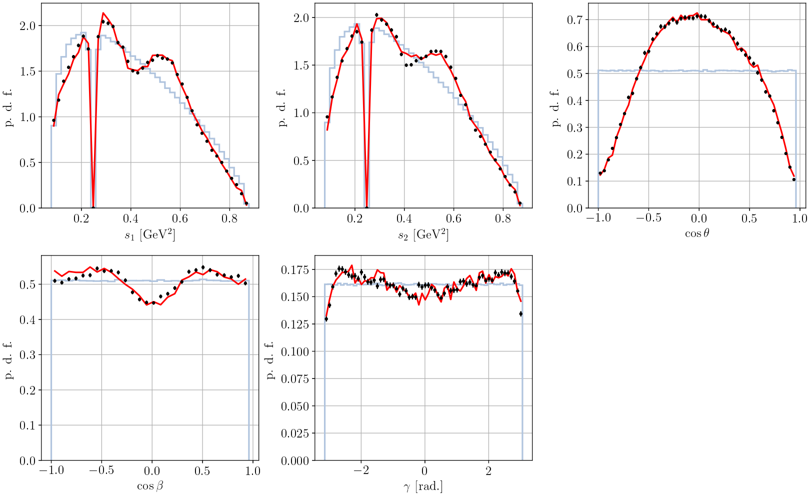

Detector resolution

$$\mathcal{I}_{w\,v}(\Phi) \to \int \mathcal{I}_{w\,v}(\Phi')\varepsilon(\Phi,\Phi')\mathrm{d}\Phi',$$

Φ — reconstructed phase space variables, Φ' — generated phase space variables

Requires MC sampling for each event

Unknown $\varepsilon(\Phi,\Phi')$

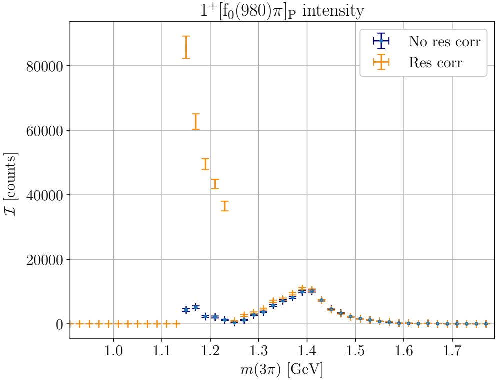

Intensity of the $1^+[\mathrm{f}_0(980)\pi]_\mathrm{P}$ wave.

Detector resolution

$$\mathcal{I}_{w\,v}(\Phi) \rightarrow \int \mathcal{I}_{w\,v}(\Phi')\varepsilon(\Phi,\Phi')\mathrm{d}\Phi',$$

Φ — reconstructed phase space variables, Φ' — generated phase space variables

Requires MC sampling for each event

Unknown $\varepsilon(\Phi,\Phi')$

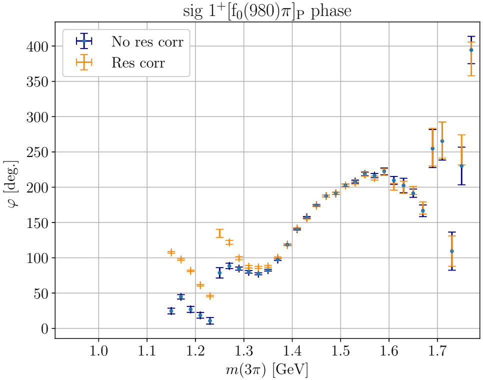

Phase of the $1^+[\mathrm{f}_0(980)\pi]_\mathrm{P}$ wave.